MinD proteins regulate CetZ1 localisation in *Haloferax volcanii*

Hannah J. Brown[1] and Iain G. Duggin[1,#]

[1]Australian Institute for Microbiology and Infection, University of Technology Sydney, Ultimo, NWS, 2007, Australia.

[#]Correspondence: iain.duggin@uts.edu.au

Abstract

CetZ proteins are archaea-specific homologues of the cytoskeletal proteins FtsZ and tubulin. In the pleomorphic archaeon *Haloferax volcanii*, CetZ1 contributes to the development of rod shape and motility. CetZ1 shows complex subcellular localization, including irregular midcell structures and filaments along the long axis of developing rods and patches at the cell poles of the motile rod cell type, where it contributes to the proper assembly and positioning of the archaellum and chemotaxis motility proteins. The polar localisations of archaellum and chemotaxis proteins are also influenced by MinD4, the only previously characterized archaeal member of the MinD family of ATPases, which are better known for their roles in the positioning of the division ring in bacteria. Using MinD mutant strains and CetZ1 localization studies, we show here that a second MinD protein, MinD2, has a strong influence on motility and the localization of CetZ1. Knockout of the *minD2* gene altered the distribution of CetZ1 in a midcell zone and along the edges of rod cells, and inhibited the localization of CetZ1 at the cell poles. MinD4 had a similar but weaker influence on motility and CetZ1 localization. The MinD2/4 mutant strains formed normal rod cell shapes like the wildtype at an early log stage of growth. Our results are consistent with distinct roles for CetZ1 in rod shape formation and at the poles of mature rods, that are positioned through the action of the MinD proteins and contribute to the development of swimming motility. They represent the first demonstration of MinD proteins controlling the positioning of tubulin superfamily proteins in archaea.

Introduction

Spatial and temporal regulation of protein subcellular localization is critical for the proper function of all cells. In bacteria, there are several different classes of proteins from the ParA/MinD family [1], which coordinate positioning of flagella [2; 3], chemosensory arrays [4; 5], chromosomes [6], plasmids [7], cell division cytoskeletal proteins [8; 9], and various other molecules or structures [10; 11; 12; 13; 14]. A key characteristic of ParA/MinD family proteins is their ATPase activity [15; 16] and dimerization [9; 17] involving amino acid residues within a deviant Walker A motif [1; 10]. In MinD proteins, this ATP binding and hydrolysis drives intracellular Min system dynamics that can generate concentration gradients of Min proteins [7; 15; 16]. In bacteria, these gradients are critical for the correct positioning of FtsZ, a key cell division protein and tubulin superfamily homologue [18; 19; 20], at mid-cell to help ensure symmetric division of the mother cell into two daughter cells [9; 21; 22].

The Min system of *Escherichia coli* is the prototypical example of Min system dynamics and function in bacteria. MinD oscillates between poles of the rod-shaped cells, controlled by its regulator MinE, and carries MinC an FtsZ antagonist. Together, these proteins generate dynamic concentration gradients of MinCD which is on average highest at cell poles and lowest at mid-cell, preventing Z-ring formation anywhere other than at mid-cell [8]. MinE accelerates the ATPase activity of MinD [15] and drives its release from the membrane which it is bound to via a membrane targeting sequence [23; 24; 25]. Together these proteins constitute a reaction-diffusion system driven by the hydrolysis of ATP. Disruption of MinD ATPase activity blocks oscillation and function completely [26; 27].

ParA/MinD family homologues have been identified across the archaeal domain, but MinD homologues are particularly abundant in *Euryarchaea* [28]. In the model halophilic archaeon, *Haloferax volcanii*, there are four MinD paralogues. The functions of MinD1-3 in have not been described and no clear protein partners equivalent to bacterial MinE have been identified. MinD4 has been characterised and is known to oscillate between cell poles, as well as concentrating with a cap-like appearance at the poles [28]. Surprisingly, the oscillation was not dependent on the ATPase Walker A or Walker B motifs, but the cap-like structures were, suggesting that the oscillation is driven by an alternative energy source [28]. Furthermore, although *H. volcanii* possess FtsZ homologues, none of the MinD paralogues were found to have a role in the mid-cell positioning of FtsZ; simultaneous deletion of all four paralogues had no detected effect of FtsZ positioning. Instead, deletion of *minD4* caused a motility defect and reduced the polar positioning of key protein constituents of the archaellum and chemotaxis arrays, ArlD and CheW, respectively [28]. Furthermore, disruption of MinD4 predicted ATPase activity through mutations to the Walker A or Walker B motifs, or truncation of its extended C-terminal tail all result in motility defects. Potential roles of the other MinD paralogues in motility of *H. volcanii* have not been reported.

Although the archaellum and chemosensory arrays are considered the core motility machinery in *H. volcanii*, there are many other contributing factors, and a range of proteins with a variety of primary functions have been shown to influence motility [29; 30; 31; 32; 33; 34; 35; 36; 37; 38]. CetZ cytoskeletal proteins, a group of tubulin superfamily proteins specific to archaea and abundant in Haloarchaea [37; 39; 40], have been implicated in the control of cell shape and motility [37; 41]. The most well-studied and highly conserved CetZ homologue, CetZ1, is necessary for rod-shape development and swimming motility [37; 41]. Our recent results have suggested that CetZ1 is an important factor for the proper assembly and positioning of motility proteins ArlD and CheW [42]. It is not yet clear whether CetZ1 contributes to motility solely via its essential role in rod shape development [37], or whether it has other functions that promote motility. It also is not yet clear how MinD4 and CetZ1 might coordinate their activities to regulate positioning and assembly of motility machinery.

Currently, no connection between Min proteins and FtsZ or other tubulin superfamily homologues, such as the CetZ, has been observed in archaea. Here, we investigate the potential for MinD homologues of *H. volcanii* to control positioning of CetZ1 and identify MinD2 as a strong regulator of CetZ1 localisation in rod cells. This is consistent with a model in which a hierarchy or network of proteins is involved the promoting the development of motility structures at the cell poles.

Methods

Growth and culturing

Haloferax volcanii was routinely grown in Hv-Cab [43] medium supplemented with uracil (50 µg/mL) to fulfil auxotrophic requirements if necessary, or L-Tryptophan (1 mM) to induce expression of genes under the control of the p.*tna* promotor. Liquid cultures were grown at 42 °C with shaking (200 rpm). Throughout this work, *H. volcanii* H26 was used as the wildtype parent strain for deletion mutants. A list of strains used in this study is provided in Table S1.

Strain and plasmid construction

To create chromosomal point mutations in *minD2*, generating strains ID810 (*minD2WA**) and ID811 (*minD2WB**), H26 was transformed with vectors pTA131_minD2WA or pTA131_minD2WB, respectively, using previously described transformation methods [44] and the 'pop-in pop-out' method [45] was used to replace the native *minD2* gene with Walker A (K16A, AAG to GCC) or Walker B (D117A, GAT to GCC) mutant alleles. Primers MinD2_USflank_extF (forward) and MinD2_DSflank_extR (reverse), designed to bind externally to the regions of homologous recombination, were then used to amplify the *minD2* locus. The resultant PCR products were purified, and then sequenced by Sanger sequencing (Australian Genome Research Facility) to identify transformants carrying the expected mutations.

Plasmids for the expression of *minD2*, *minD2WA**, and *minD2WB** were generated by amplifying these open reading frames from *H. volcanii* H26 (ID621), ID810, and ID811, respectively. Forward and reverse primers for this reaction incorporated NdeI and BamHI restriction sites at 5' and 3' ends, respectively. ORFs were then ligated between the same restriction sites in pTA962 [46], generating pHJB63-65 which were sequence verified. Plasmids and oligonucleotides used in this study are listed in Table S2 and S3, respectively.

Soft-agar motility assays

Soft-agar motility assays were carried out as described in [42], using Hv-Cab with 0.25% (w/v) agar and 1 mM L-Tryptophan. Motility was quantified by averaging perpendicular measurements of the motility halo diameter after three days of incubation of the plates inside a plastic bag at 42 °C.

Light microscopy

To prepare samples for microscopy, single colonies were first used to inoculate 3 mL Hv-Cab medium, and these cultures were allowed to grow to OD_{600} ~0.6. Then, 3 µL of this culture was taken to inoculate 10 mL Hv-Cab supplemented with 1 mM L-Tryptophan and

grown for 18 h (OD_{600} ~ 0.1). A 2 µL droplet of cells was spotted onto a 1.5% agarose pad containing 18% BSW as described in [37]. Samples were then covered with a clean #1.5 glass coverslip.

Imaging for phase-contrast and fluorescence microscopy was carried out using a V3 DeltaVision Elite (GE Healthcare) with an Olympus UPLSAPO 100X NA 1.4 objective and pco.edge 5.5 sCMOS camera. A filter set for mTurquoise2/CFP (excitation=400-453, emission=463-487) was used for imaging of CetZ1-mTq2 expressing strains. 3D Structured-illumination microscopy (3D-SIM) was conducted as described previously [41] using a DeltaVision OMX SR microscope (GE Healthcare) and a DAPI filter for excitation (405 nm) and an AF488 filter for emission (504-552 nm), suitable for imaging of mTurquoise2. Raw images were reconstructed using SoftWorx (Applied Precision, GE Healthcare), and 3D renders were generated [47]using Bitplane IMARIS (v9.6.0).

Image analysis

Image analysis was conducted using the MicrobeJ (v5.13I) [48] plugin for FIJI (v2.14.0/1.54f) [49]. Cell shape characteristics were analysed using phase-contrast images and default settings. Fluorescent foci detection was carried out after background subtraction with a ball size of 50 pixels, and the *point* detection method was used for analysis of CetZ1-mTq2 localisation (Tolerance=200).

Fluorescence intensity profiles along the long axis of each cell were generated using the *XStatProfile* function in MicrobeJ (the long axis was normalized between 0-1). The mean and standard deviation of the raw fluorescence intensity over all cells were then determined (Stat=mean±stdv, Y axis=MEDIAL.intensity.ch2, number of bins=50). The intensity data were also normalized (0-100%) and the median fluorescence intensity along the long axis determined for each culture replicate (Stat=median, Y axis=MEDIAL.intensity.ch2, number of bins=50), and then the mean and standard error of all culture replicates were plotted. These data were also displayed as the difference in fluorescence intensity between *minD* deletion or Walker mutant backgrounds and the wildtype background.

Heatmaps of foci localisation were generated using the *XYCellDensity* function (Rendering=Density) with default settings.

Results

MinD2 knockout shows a strong motility defect and can form normal rod cell shapes

We began by assessing the effect of MinD2 and MinD4 gene deletions on motility. These are the two MinD paralogues of *H. volcanii* that are expressed significantly in standard culture conditions [50; 51; 52]. Motility was assessed using soft-agar motility assays, in which cells develop into a motile rod form [37] and then swim out through the gel from a central inoculation point, forming a halo. All the *H. volcanii* strains analysed here contained a pHV2-based vector (pTA962 vector or derivatives) to complement the *pyrE2* auxotrophic marker in the host strain H26 (Δ*pyrE2* ΔpHV2) and better match the original *H. volcanii* wild-type genotype; previous work has shown that the base strains with Δ*pyrE2*, Δ*hdrB* or ΔpHV2 show poorer expression of the cell morphology and motility phenotypes, which are sensitive to nutrient and culture conditions [37; 43; 53].

Deletion of *minD2* resulted in a motility defect (approximately 25% of the halo diameter compared to wildtype), which was significantly stronger than that caused by deletion of *minD4* (approximately 50% of wildtype motility) (Fig. 1a, b). Deletion of both *minD2* and *minD4* resulted in a stronger motility defect (approximately 16% of wildtype motility). The deletion of all four *minD* homologues (Δ*minD1/2/3/4*) was equivalent to that of the Δ*minD2/4* indicating that MinD1 and MinD3 do not have substantial roles in the standard motility conditions tested here.

H. volcanii is pleomorphic and cultures can show a range of cell shapes including irregular disk, or plate-shaped cells, and rods with varying widths and degrees of elongation [37; 43]. Furthermore, a motile-rod cell type with regular cell widths develops under certain conditions to promote swimming [37; 54]. To determine whether the two MinD proteins are required for rod formation, which might contribute to their effects on motility, we sampled wild-type and Δ*minD2/4* cells from the early-log phase of liquid batch cultures (OD ~ 0.1), where motile rods are prevalent [43; 54]. By quantifying cell circularity as an indicator of the extent of cell elongation, we observed no significant cell shape differences at this stage of growth in any of the strains (Fig. 1c, d).

MinD2 and MinD4 influence the cellular positioning of CetZ1

MinD4 has been shown to have a role in the polar positioning of the archaellum and chemotaxis arrays, through the use of tagged marker proteins ArlD and CheW, respectively [28]. We recently found that CetZ1 also influences the proper assembly and positioning of ArlD and CheW [42]. It is unknown whether MinD4 and CetZ1 cooperate or work independently to promote motility. To begin investigating this, we sought to determine whether MinD2 or MinD4 regulate the localisation of CetZ1.

To do this, we observed the localisation of a CetZ1-mTurquoise2 (mTq2) fusion protein [55] in the various *minD* deletion strain backgrounds. Fluorescence microscopy of CetZ1-

194 mTq2 (Fig. 2a) in wildtype cells imaged in early-log growth (OD_{600} ~ 0.1), showed the
195 expected patchy localisation with relatively high fluorescence at cell poles and the mid-
196 cell region [41; 42; 55]. In the Δ*minD2* background, CetZ1-mTq2 localisation remained
197 patchy and concentrated in a broad zone near mid-cell, but the high-intensity polar
198 localisations of CetZ1-mTq2 were not observed (e.g., Fig. 2a). We investigated this
199 quantitatively by image analysis of larger numbers of cells. This included heatmaps of the
200 position and frequency of fluorescent foci in cells (Fig. 2b), and plots showing the total
201 and normalized mean fluorescence intensity of CetZ1-mTq2 along the long-axis of the
202 cells (Fig. 2c-e). These results displayed clear peaks of fluorescence at the cell poles in
203 the wildtype background, but almost complete loss of these peaks at the cell poles in the
204 Δ*minD2* background. A weaker defect of CetZ1-mTq2 polar localization was also
205 observed in the Δ*minD4* background (compare the polar intensities between mutant and
206 wildtype in Fig. 2d). Additional control experiments demonstrated that the Δ*minD* strains
207 producing CetZ1-mTq2 had no significant differences in shape compared to the wildtype
208 control (OD ~ 0.1), and we also observed an equivalent motility defect with or without the
209 CetZ1-mTq2 fusion (Fig. S1a).

210 The results in Fig. 2 also revealed that the zone of CetZ1-mTq2 localization around the
211 midcell region was broadened in the absence of either MinD2 or MinD4 (Fig. 2b, d, e).
212 Interestingly, such broadening was not apparent in strains in which both *minD2* and
213 *minD4* were deleted, although the polar localization of CetrZ1-mTq2 was still strongly
214 inhibited (Fig. 2b, d, e). This suggests that the midcell zone of CetZ1-mTq2 localization is
215 impacted when only one of MinD2 or MinD4 is present and implies a genetic interaction
216 or interference between *minD2* and *minD4* that influences midcell CetZ1.

217 We further resolved the CetZ1-mTq2 polar localizations and the effects of the MinD
218 knock-outs by three-dimensional structured-illumination microscopy (3D-SIM); 3D
219 reconstructions were visualized as maximum intensity projections viewed down the z-
220 plane (Fig. 3a), and via 3D rendering (Fig. 3d, 3e, Supplementary Video 1-4). In wildtype
221 early-log cells (Fig. 3a), CetZ1-mTq2 often appeared as a bright focus, doublet, multi-
222 lobed, or cap-like structure at the cell poles, suggestive of a ring or disc-like structure at
223 the tip of the cell pole. In the absence of MinD2, the foci of CetZ1-mTq2 appeared more
224 randomly distributed around the whole cell, with no clear preference for the cell poles
225 (Fig. 3b). In the absence of MinD4, this effect was weaker, and some of the cells still
226 appeared to show the relatively bright polar tip structures of CetZ1-mTq2 (Fig. 3c). The
227 Δ*minD4* cells also showed more of the CetZ1-mTq2 patches throughout the cell than the
228 wildtype, consistent with the observed broadening of the midcell zone (Fig. 2b, d, e). The
229 relative effects of MinD2 and MinD4 on CetZ1-mTq2 localization approximately
230 correlated with the magnitude of their impacts on motility (Fig. 1 and 2).

231 ***ATPase active-site residues of MinD2 are required for normal swimming motility and***
232 ***polar localization of CetZ1***

MinD proteins typically rely on ATP hydrolysis to drive their dynamic localization patterns, such as oscillation between cell poles, generating concentration gradients which form the basis for their spatial and temporal control of downstream proteins [10; 27; 28]. When the Walker A and Walker B motifs of *H. volcanii* MinD4 were previously mutated to disrupt ATP binding and hydrolysis, swimming motility was reduced and polar localisation of MinD4 was disrupted, although not its oscillation [28].

Given that MinD2 had the strongest effects on swimming motility and CetZ1 polar localisation, we chose to further investigate the importance of the ATPase active-site for MinD2 functionality in motility and CetZ1 localization. We generated chromosomal point-mutations in the endogenous *minD2* gene in the ATPase active site via the deviant Walker A (K16A) and Walker B (D117A) motifs, here forth referred to as *minD2WA** and *minD2WB**, respectively. These mutations are equivalent to those previously made in MinD4 [28].

Both *minD2WA** and *minD2WB** strains (containing the empty vector pTA962) partially perturbed motility, resulting in ~78% and ~36% of the wildtype motility halo diameter, respectively (Fig. 4a, c), compared to the complete deletion of *minD2* (~25%, Fig. 1a, b). The motility defect of Δ*minD2* was complemented by expressing *minD2* from a plasmid (pTA962 backbone), confirming the important role of *minD2* in motility (Fig. 4b, c). When *minD2WA** was expressed from a plasmid in the Δ*minD2* background, this strain had a more pronounced motility defect (~35%) compared to the chromosomal mutant *minD2WA** (~78%). On the other hand, expression of *minD2WB** from pTA962 in *ΔminD2* produced equivalent motility to the complete *minD2* deletion, consistent with its much stronger effects on motility observed with the chromosomal *minD2WB** mutant (Fig. 4b, c).

Phase-contrast microscopy and quantification of cell shape (circularity) confrimed that, like Δ*minD2*, the Walker A and Walker B mutations did not significantly affect rod shape (at OD ~0.1), whether expressed chromosomally (Fig. S2a, c) or from the plasmid (Fig. S2b, d). We then assessed the effect of the *minD2WA** and *minD2WB** chromosomal mutants on CetZ1-mTq2 localisation. Control experiments showed that expression of CetZ1-mTq2 did not impact cell circularity or motility of either the *minD2WA** or *minD2WB** strains (Fig. S1c, d). Fluorescence microscopy (Fig. 5a) showed that both Walker mutations resulted in a substantial loss of CetZ1-mTq2 fluorescence intensity (Fig. 5c, dc) and foci localisation at cell poles and showed the midcell zone broadening (Fig. 5b) like in the Δ*minD2* background (Fig. 2).

Discussion

MinD proteins and related protein families are important for spatial and temporal positioning of a variety of molecules but have mainly been characterized in bacteria [10]. One of four MinD paralogues in the archaeal model organism *H. volcanii*, MinD4, has previously been described to affect motility via regulating the positioning of archaellum and chemotaxis arrays, via unknown mechanisms [28]. The tubulin-like cytoskeletal protein CetZ1 is another factor promoting the proper assembly and positioning of these proteins at the cell poles, where it is hypothesised to form a scaffold-like structure [42].

We found here that MinD2 is important for motility and for the subcellular positioning of CetZ1. Deletion of *minD2* was found to have a more severe motility defect than deletion of *minD4*, and deletion of both genes resulted in an even greater motility defect, suggesting distinct roles or additive contributions of these two MinD paralogues in motility. MinD2 and to a lesser extent MinD4 also influenced the subcellular positioning of CetZ1 in the midcell region and at the poles. The polar-localised CetZ1 has no essential role in maintaining rod shape, because *ΔminD2* cells could still form normal shaped rods, despite the strong loss of CetZ1 at the poles. CetZ1 may have distinct roles in establishing rod-shape during the earlier stages of motile rod cell differentiation [37], and then at the poles of the mature motile rods.

We found that mutations in the Walker A and B motifs of the MinD2 ATPase both strongly blocked CetZ1 polar positioning, like *minD2* deletion. However, only the Walker B mutant (D117A) strongly perturbed motility, whereas the Walker A (K17A) mutant (in its chromosomal context) resulted in only a milder motility defect. This may suggest that MinD2 has an impact on motility that is independent of the K17 residue and polar CetZ1 positioning. The K17 residue is expected to be involved in nucleotide dependent dimerization [27], so this function may not be critical to the motility function of MinD2, though we found it is important for CetZ1 polar localization. In contrast, the equivalent MinD4 Walker A and B mutants reduced motility equivalently to *minD4* deletion [28].

The accompanying study by Patro et al. [56] found that MinD2 is required for normal motility and the proper polar localisation of ArlD and CheW, like MinD4 [28]. They also reported a delayed development of rod cells during the early log phase in the Δ*minD2* compared to the wildtype. This likely represents an earlier phase of *H. volcanii* cultures, where cells are actively shapeshifting into motile rods [43; 54], compared to the early log sampling time in the current study where those rods had already formed and we found that their cell shapes in the wildtype and Δ*minD2* strains were indistinguishable. Though we note that since *H. volcanii* morphogenesis is highly sensitive to exact media composition and culture conditions [43; 53], excessive comparisons of the exact magnitudes or timing of events from separate studies should be avoided.

Considering the main findings from recent studies, the results of the current study imply that MinD2 and MinD4 might help place the archaellum and chemotaxis proteins at the

cell poles via positioning and assembly of polar CetZ1, which in turn contributes to the proper assembly and positioning of the archaellum and chemotaxis arrays as we recently observed [42]. However, the finding that the chromosomal *minD2WA** blocked polar CetZ1 localization but only weakly affected motility would argue that polar CetZ1 is not critical for motility and thus may not be how MinD2 is delivering its influence on motility. Alternatively, MinD2 and MinD4 might separately control the position of CetZ1 and the motility machinery at the cell poles (Fig. 6). Finally, MinD2 could also act on the timing of rod development (potentially via CetZ1), potentially impacting Arl/Che placement at poles [56] with subsequent consequences for motility. These possibilities are not mutually exclusive, and the resolution of the pathways and mechanisms involved should be of interest in future.

In summary, our findings showed that multiple MinD homologues can have differing functions and regulate the subcellular positioning of the archaeal tubulin-like protein CetZ1 in the context of the development of swimming motility. They represent the first demonstration of MinD proteins controlling the position of tubulin superfamily proteins in archaea. The MinD-controlled positioning of CetZ1 in distinct subcellular locations is consistent with multiple functions of CetZ1, evoking parallels with the multiple functions of tubulins and other eukaryotic cytoskeletal proteins that are extensively regulated in time and space.

Acknowledgements

The authors would like to acknowledge facilities support from L. Cole and A. Bottomley and the UTS Microbial Imaging Facility. The work was supported by the Australian Research Council (DP160101076 and FT160100010 to IGD).

Author Contributions

Conceptualisation – HJB & IGD; Data curation - HJB; Formal Analysis – HJB; Investigation – HJB; Methodology – HJB & IGD; Supervision – IGD; Original draft – HJB; Revision and reviewing the manuscript – HJB & IGD; Funding Acquisition – IGD.

Figures

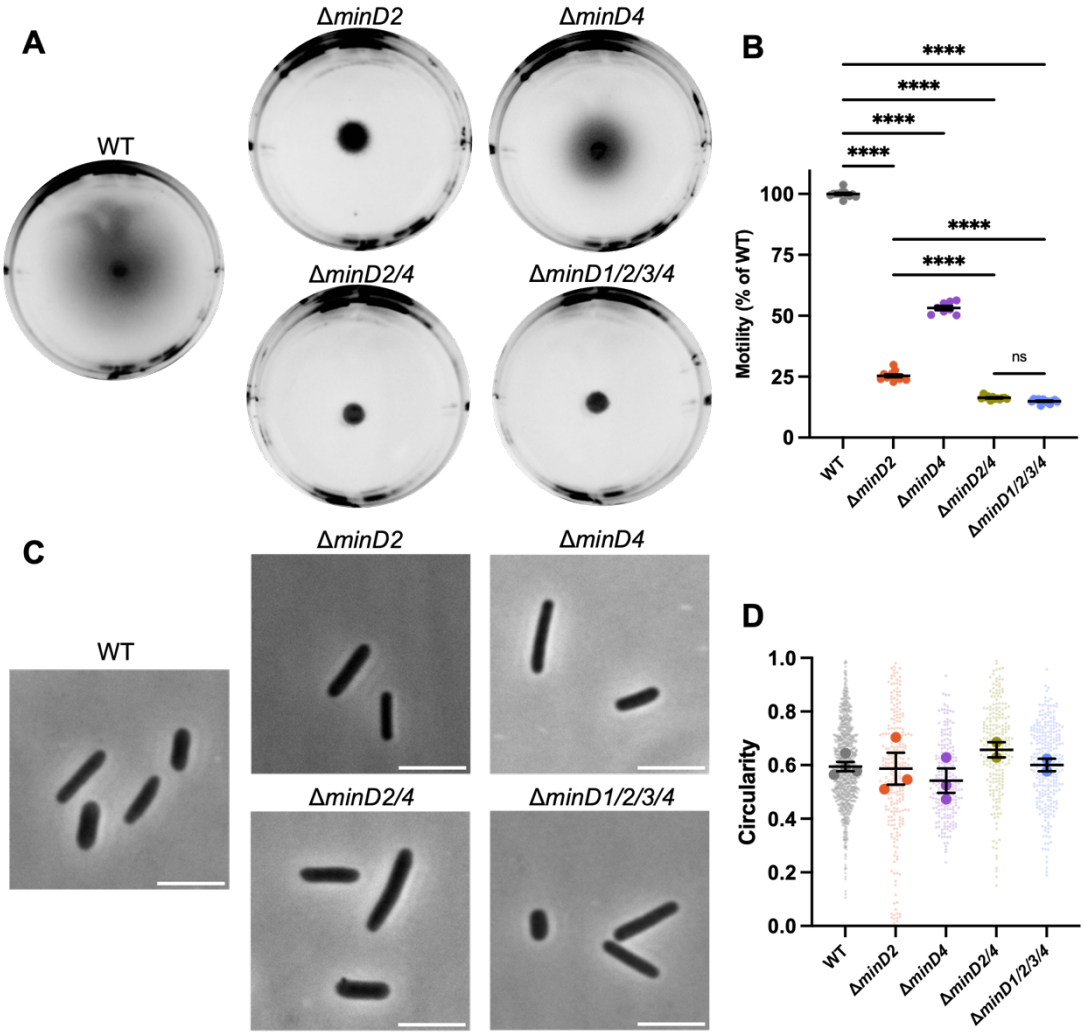

Figure 1. MinD2 and MinD4 have roles in motility without influencing shape. A) H26 wildtype and *minD* deletion mutant backgrounds, carrying an empty pTA962 vector, were use to inoculate the centre of a soft agar plate. **B)** The diameter of their motility halos was measured across six independent liquid starter culture replicates (represented by individual points), each determined from the mean of at least two replicate agar plates. Mean and standard error is shown. **C)** Phase-contrast microscopy of cells grown in Hv-Cab liquid medium with 1 mM L-tryptophan, sampled at OD_{600} ~ 0.1. Scale bars = 5 µm. **D)** Cell circularity distributions, quantified from phase-contrast images as a proxy for cell elongation. Large data points represent mean circularity of one culture replicate, small data points represent individual cells from all culture replicates for the indicated strain. Mean and standard error of culture replicate means are shown (bars). The number of individual cells measured from pooled culture replicates were as follows: WT + pTA962, n=996; Δ*minD2* + pTA962, n=247; Δ*minD4* + pTA962, n=217; Δ*minD2/4* + pTA962, n=223; Δ*minD1/2/3/4* + pTA962, n=279. In **B** and **D**, one-way ANOVA was used as a statistical test, and only significant and/or relevant comparisons are shown. ****$p<0.00005$, ns=not significant.

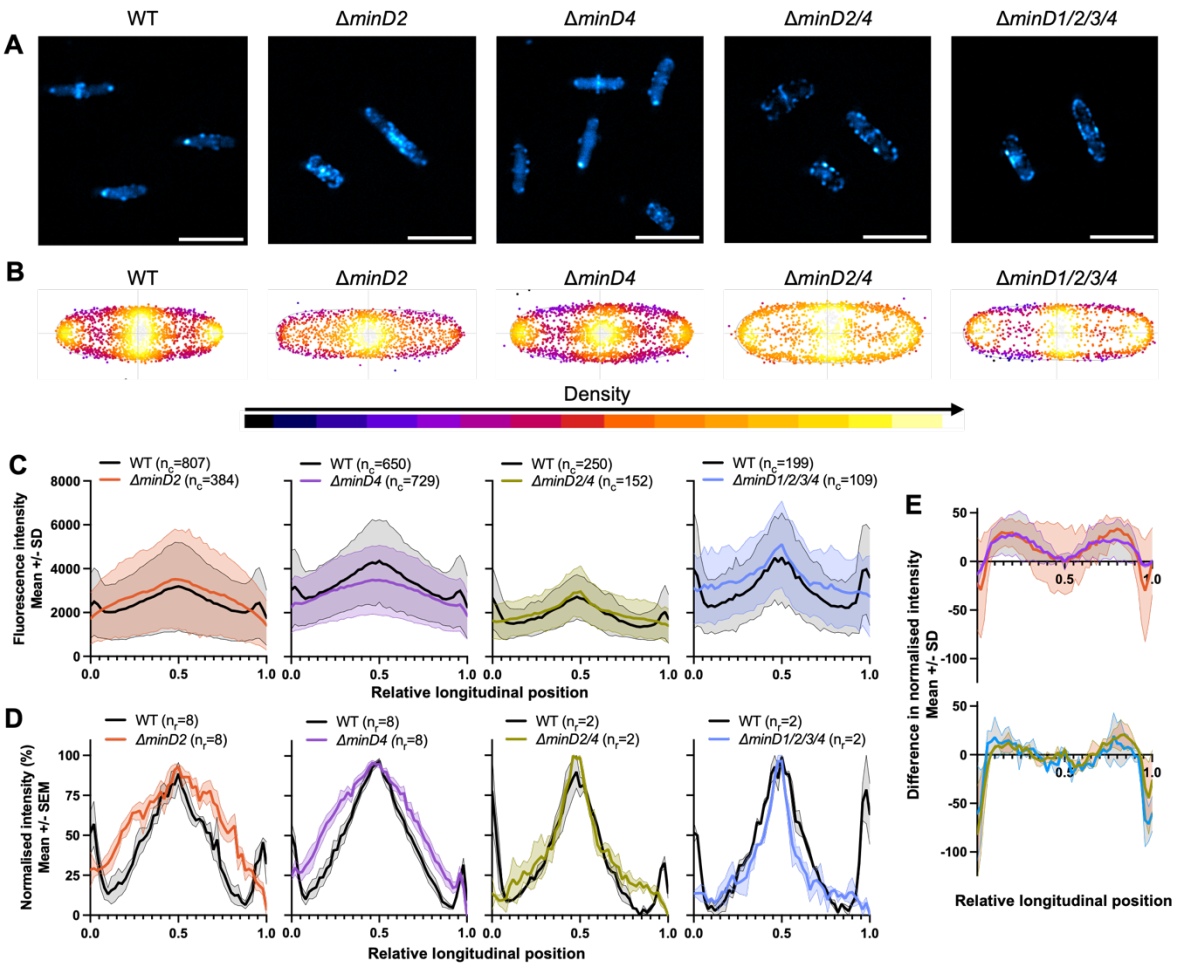

Figure 2. MinD2 controls polar positioning of CetZ1. H26 wildtype and *minD* deletion strains containing pHVID135 (for expression of CetZ1-mTq2) were grown in Hv-Cab with 1 mM L-Tryptophan and sampled at an approximate OD_{600} of 0.1. **A)** Epifluorescence images of CetZ1-mTq2 localisation in the indicated *minD* knockout strains (scale bar 5 µm). **B)** Heatmaps representing the position and number (heatmap density) of detected CetZ1-mTq2 fluorescence peak intensities (foci) along the long (vertical) and lateral (horizontal) axes of all cells combined. **C)** The median fluorescence intensity of CetZ1-mTq2 along the normalized long axis of each cell was used to generate a plot of the mean (bold line) and standard deviation (shading) of the raw fluorescence intensity data from all cells (n_c) (combined from at least two replicate cultures). Cultures of the wildtype strain were repeated in parallel alongside each mutant independently. **D)** The same intensity data in **C** were also normalized (0-100%) for each culture replicate and plotted as the mean (bold line) and standard error (shading) of all culture replicates (n_r). **E**) The difference between normalised fluorescence of each Δ*minD* strain from its wildtype control in **D** is shown as the mean (bold line) and standard deviation (shading). The key from **D** also applies to **E.**

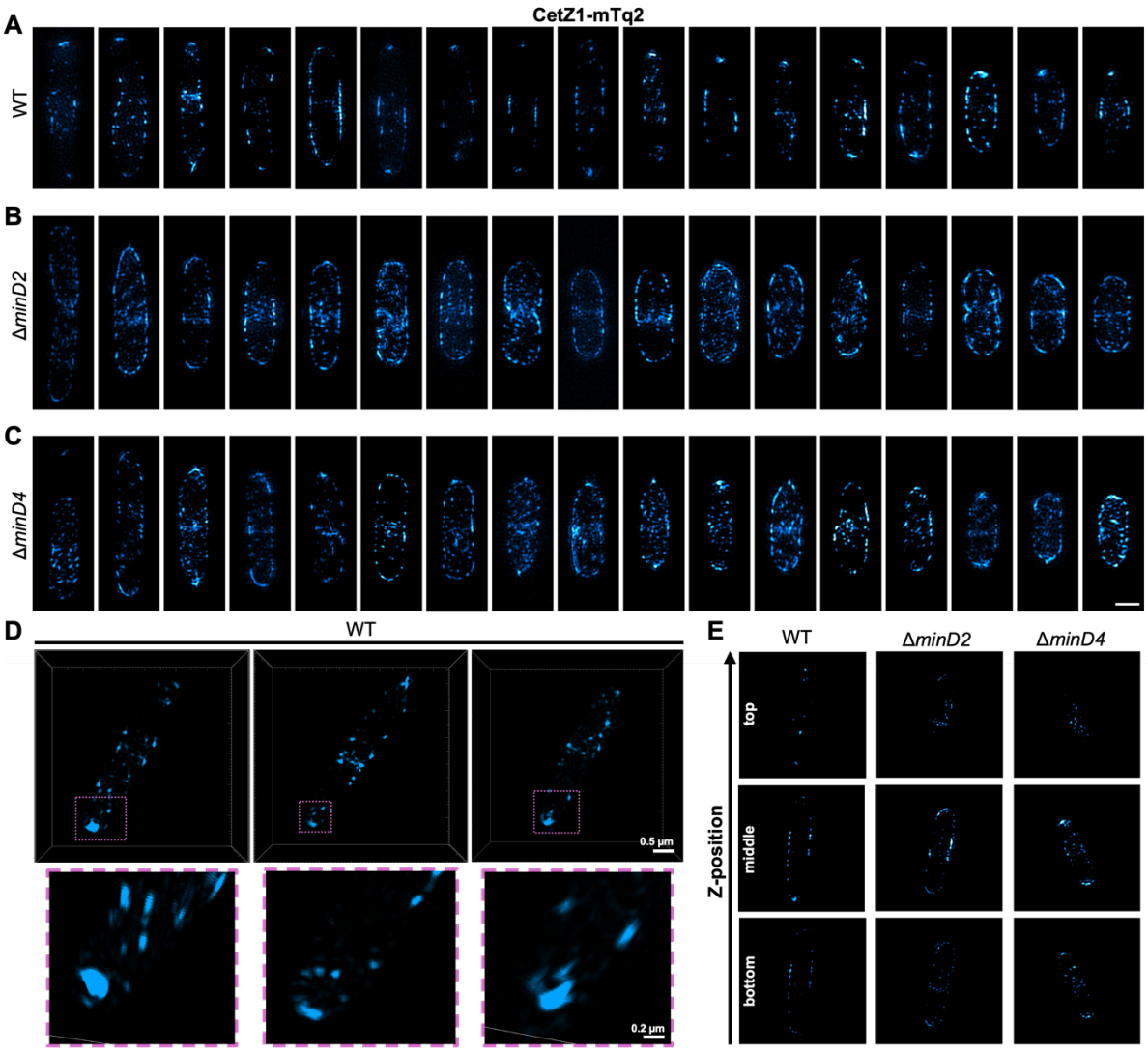

Figure 3. 3D-SIM imaging of CetZ1-mTq2. **(A-C)** Maximum intensity projections of CetZ1-mTq2 in H26 wildtype, Δ*minD2*, and *minD4* backgrounds, viewed along the imaging z-axis. Scale bar in panel C is 1 µm and applies to panels A-C. **D)** 3D rendered images, showing non-circular fluorescence foci of CetZ1-mTq2 at the cell poles in H26 wildtype background. Pink outlines indicate zoomed area (bottom). **E)** 3D rendered images showing slice sections of CetZ1-mTq2 localisation in the indicated strains at approximate bottom, middle, and top z-positions of the cells.

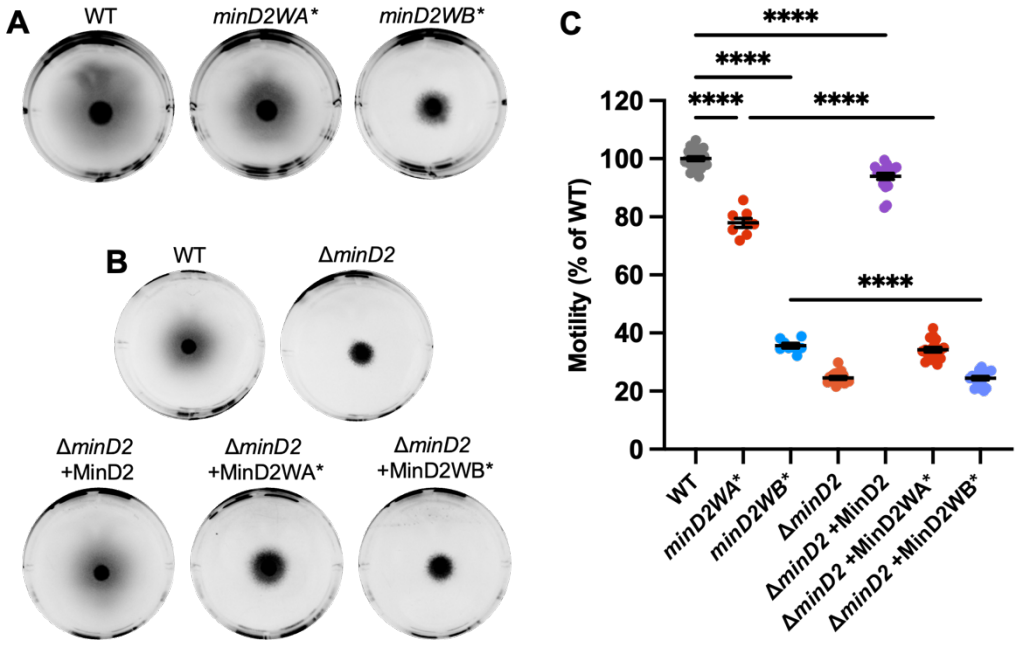

Figure 4. Chromosomal Walker mutants of MinD2 perturb motility. A) H26 wildtype, *minD2WA**, and *minD2WB** backgrounds containing pTA962, **B)** and Δ*minD2* containing pTA962 were compared to Δ*minD2* containing pHJB63-65 for expression of *minD2*, *minD2WA**, and *minD2WB**, respectively, and inoculated onto Hv-Cab soft agar (0.25 % w/v) supplemented with 1 mM L-Tryptophan. **C)** Halo diameters were quantified across four starter culture replicates with two technical replicates (motility agar plates) each (indicated by individual points). Mean and standard error are shown. One-way ANOVA was used as a statistical test, and only significant and relevant comparisons are shown. ****$p<0.00005$.

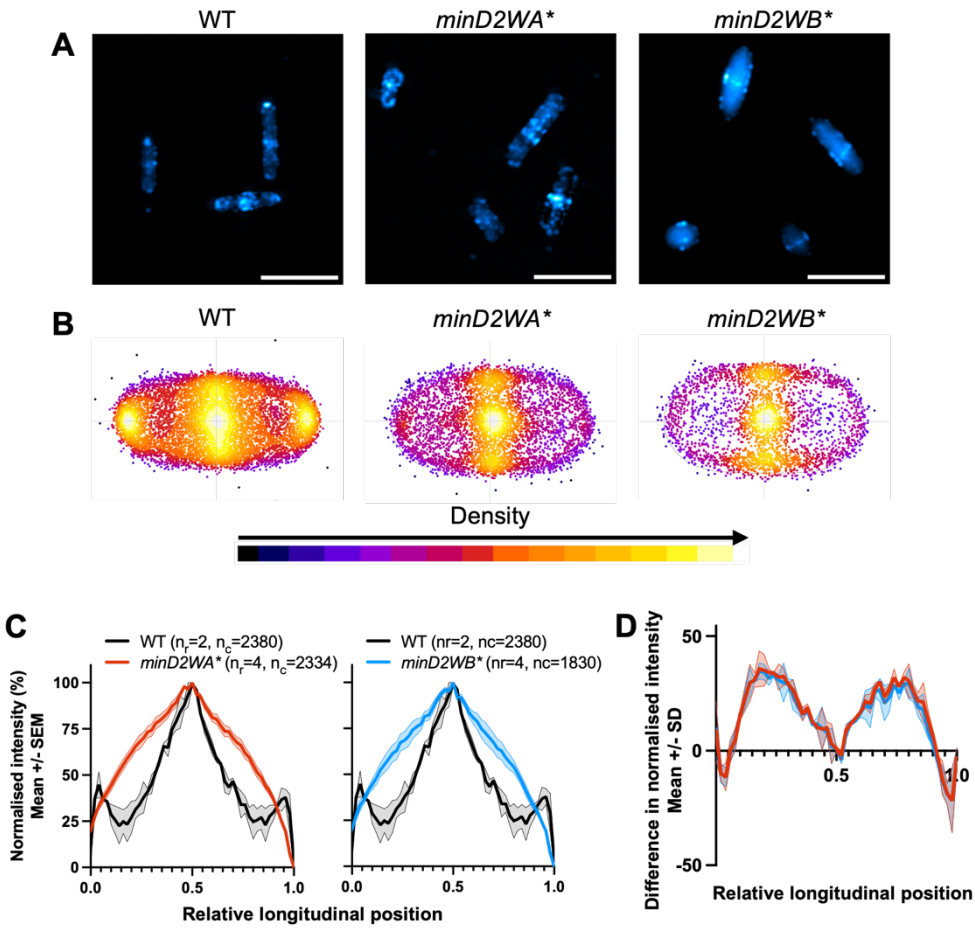

Figure 5. Chromosomal Walker mutants of MinD2 disrupt polar localisation of CetZ1. H26 wildtype and *minD2* walker mutant strains containing pHVID135 (for expression of CetZ1-mTq2) were grown in Hv-Cab with 1 mM L-Tryptophan and sampled at OD_{600} ~ 0.1. **A)** Cells were imaged using epifluorescence to observe CetZ1-mTq2 localisation. Scale bar 5 µm. **B)** Heat map representations of detected foci of CetZ1-mTq2 and their localisations. Heatmaps are coloured by density, referring to subcellular localisation along the relative length of lateral and longitudinal axes only and do not fluorescence intensity. **C)** normalised median fluorescence intensity of CetZ1-mTq2 along the long axis of the cell, represented as the mean (bold line) and standard deviation (shading) of biological replicates (as in Fig. 2d). Two biological replicates were carried out for the wildtype background, and four for each of *minD2WA** and *minD2WB**, and data for H26 wildtype is included on both graphs for reference. **D)** The difference between normalised fluorescent signals was calculated by subtracting the curve of each *minD2* walker mutant strain from the curve of the wildtype control shown in **C** and is represented as mean (bold line) and standard deviation (shading). The key from **C** also applies to **D**. The number of cells measured from pooled biological replicates in **C** and **D** are as follows: WT + CetZ1-mTq2, n=2380; *minD2WA** + CetZ1-mTq2, n=2334; *minD2WB** + CetZ1-mTq2, n=1830.

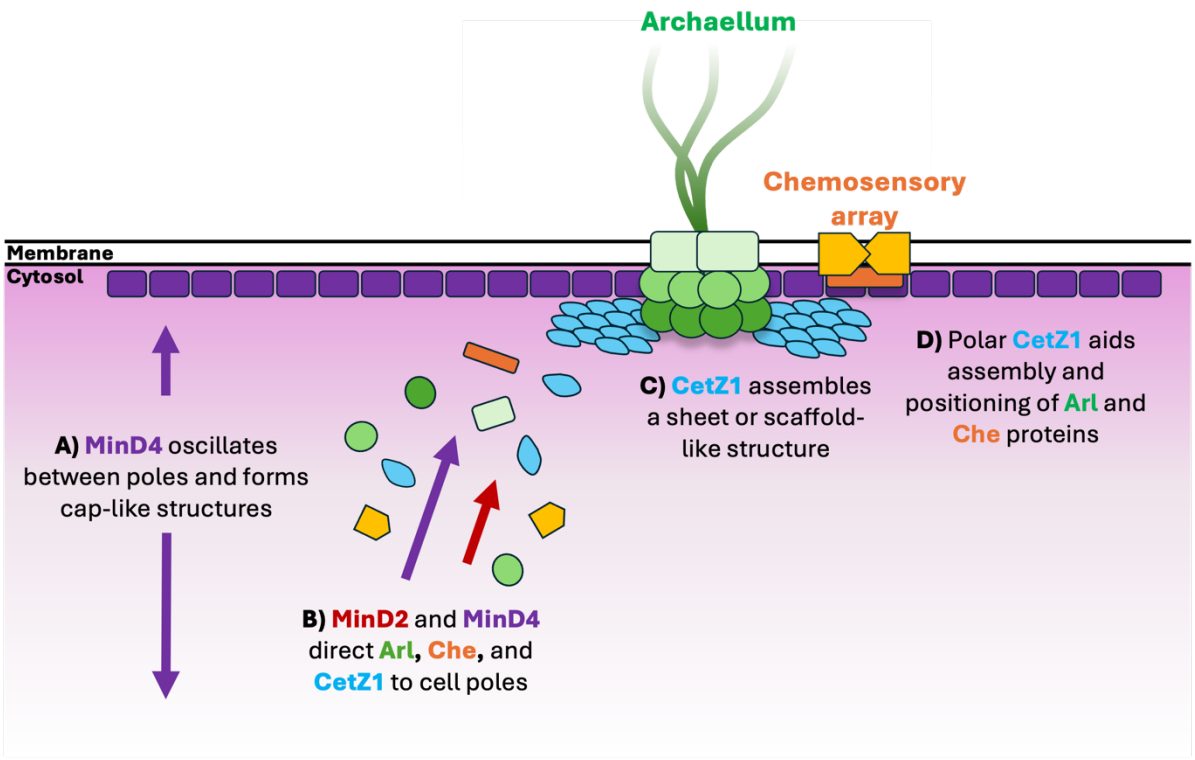

Figure 6. Schematic model for assembly of motility proteins at cell poles. A) MinD4 oscillates between cell poles and forms cap-like localisations at cell poles in an ATPase dependent manner [28]. **B)** MinD4 and MinD2 direct ArlD and CheW to cell poles. CetZ1 is also directed to cell poles, likely by both MinD paralogues, but more dominantly by MinD2. **C)** At cell poles, CetZ1 is hypothesised to assemble as a sheet or disc-like structure, **D)** where it contributes to assembly and positioning of motility structures [42].

References

[1] D.D. Leipe, Y.I. Wolf, E.V. Koonin, and L. Aravind, Classification and evolution of P-loop GTPases and related ATPases. Journal of molecular biology 317 (2002) 41-72.

[2] J.S. Schuhmacher, K.M. Thormann, and G. Bange, How bacteria maintain location and number of flagella? FEMS microbiology reviews 39 (2015) 812-822.

[3] J.S. Schuhmacher, F. Rossmann, F. Dempwolff, C. Knauer, F. Altegoer, W. Steinchen, A.K. Dörrich, A. Klingl, M. Stephan, and U. Linne, MinD-like ATPase FlhG effects location and number of bacterial flagella during C-ring assembly. Proceedings of the National Academy of Sciences 112 (2015) 3092-3097.

[4] S. Ringgaard, K. Schirner, B.M. Davis, and M.K. Waldor, A family of ParA-like ATPases promotes cell pole maturation by facilitating polar localization of chemotaxis proteins. Genes & Development 25 (2011) 1544-1555.

[5] M.A. Roberts, G.H. Wadhams, K.A. Hadfield, S. Tickner, and J.P. Armitage, ParA-like protein uses nonspecific chromosomal DNA binding to partition protein complexes. Proceedings of the National Academy of Sciences 109 (2012) 6698-6703.

[6] A.S. Jalal, and T.B. Le, Bacterial chromosome segregation by the ParABS system. Open biology 10 (2020) 200097.

[7] J.C. Baxter, and B.E. Funnell, Plasmid partition mechanisms. Plasmids: biology and impact in biotechnology and discovery (2015) 133-155.

[8] J. Lutkenhaus, Assembly dynamics of the bacterial MinCDE system and spatial regulation of the Z ring. Annu. Rev. Biochem. 76 (2007) 539-562.

[9] Z. Hu, and J. Lutkenhaus, Topological regulation of cell division in E. coli: spatiotemporal oscillation of MinD requires stimulation of its ATPase by MinE and phospholipid. Molecular cell 7 (2001) 1337-1343.

[10] J. Lutkenhaus, The ParA/MinD family puts things in their place. Trends in microbiology 20 (2012) 411-418.

[11] B.A. Perez-Cheeks, P.J. Planet, I.N. Sarkar, S.A. Clock, Q. Xu, and D.H. Figurski, The product of tadZ, a new member of the parA/minD superfamily, localizes to a pole in Aggregatibacter actinomycetemcomitans. Molecular microbiology 83 (2012) 694-711.

[12] G. Laloux, and C. Jacobs-Wagner, How do bacteria localize proteins to the cell pole? Journal of cell science 127 (2014) 11-19.

[13] S.R. Thompson, G.H. Wadhams, and J.P. Armitage, The positioning of cytoplasmic protein clusters in bacteria. Proceedings of the National Academy of Sciences 103 (2006) 8209-8214.

[14] D.F. Savage, B. Afonso, A.H. Chen, and P.A. Silver, Spatially ordered dynamics of the bacterial carbon fixation machinery. Science 327 (2010) 1258-1261.

[15] M. Loose, E. Fischer-Friedrich, C. Herold, K. Kruse, and P. Schwille, Min protein patterns emerge from rapid rebinding and membrane interaction of MinE. Nature structural & molecular biology 18 (2011) 577-583.

[16] M. Howard, and K. Kruse, Cellular organization by self-organization: mechanisms and models for Min protein dynamics. The Journal of cell biology 168 (2005) 533.

[17] T.D. Dunham, W. Xu, B.E. Funnell, and M.A. Schumacher, Structural basis for ADP-mediated transcriptional regulation by P1 and P7 ParAn. The EMBO journal 28 (2009) 1792-1802.

[18] E. Bi, K. Dai, S. Subbarao, B. Beall, and J. Lutkenhaus, FtsZ and cell division. Research in microbiology 142 (1991) 249-252.
[19] H.P. Erickson, FtsZ, a prokaryotic homolog of tubulin? Cell 80 (1995) 367-370.
[20] E. Nogales, K.H. Downing, L.A. Amos, and J. Löwe, Tubulin and FtsZ form a distinct family of GTPases. Nature Structural and Molecular Biology 5 (1998) 451.
[21] D.M. Raskin, and P.A. De Boer, Rapid pole-to-pole oscillation of a protein required for directing division to the middle of Escherichia coli. Proceedings of the National Academy of Sciences 96 (1999) 4971-4976.
[22] P.A. De Boer, R.E. Crossley, and L.I. Rothfield, A division inhibitor and a topological specificity factor coded for by the minicell locus determine proper placement of the division septum in E. coli. Cell 56 (1989) 641-649.
[23] L.L. Lackner, D.M. Raskin, and P.A. De Boer, ATP-dependent interactions between Escherichia coli Min proteins and the phospholipid membrane in vitro. Journal of bacteriology 185 (2003) 735-749.
[24] K.-T. Park, W. Wu, K.P. Battaile, S. Lovell, T. Holyoak, and J. Lutkenhaus, The Min oscillator uses MinD-dependent conformational changes in MinE to spatially regulate cytokinesis. Cell 146 (2011) 396-407.
[25] T.H. Szeto, S.L. Rowland, L.I. Rothfield, and G.F. King, Membrane localization of MinD is mediated by a C-terminal motif that is conserved across eubacteria, archaea, and chloroplasts. Proceedings of the National Academy of Sciences 99 (2002) 15693-15698.
[26] H. Zhou, R. Schulze, S. Cox, C. Saez, Z. Hu, and J. Lutkenhaus, Analysis of MinD mutations reveals residues required for MinE stimulation of the MinD ATPase and residues required for MinC interaction. Journal of bacteriology 187 (2005) 629-638.
[27] J. Lutkenhaus, and M. Sundaramoorthy, MinD and role of the deviant Walker A motif, dimerization and membrane binding in oscillation. Molecular microbiology 48 (2003) 295-303.
[28] P. Nußbaum, S. Ithurbide, J.C. Walsh, M. Patro, F. Delpech, M. Rodriguez-Franco, P.M. Curmi, I.G. Duggin, T.E. Quax, and S.-V. Albers, An oscillating MinD protein determines the cellular positioning of the motility machinery in archaea. Current Biology 30 (2020) 4956-4972. e4.
[29] M. Tripepi, S. Imam, and M. Pohlschröder, Haloferax volcanii flagella are required for motility but are not involved in PibD-dependent surface adhesion. Journal of bacteriology 192 (2010) 3093-3102.
[30] M. Tripepi, J. You, S. Temel, Ö. Önder, D. Brisson, and M. Pohlschröder, N-glycosylation of Haloferax volcanii flagellins requires known Agl proteins and is essential for biosynthesis of stable flagella. Journal of bacteriology 194 (2012) 4876-4887.
[31] M.F. Abdul Halim, F. Pfeiffer, J. Zou, A. Frisch, D. Haft, S. Wu, N. Tolić, H. Brewer, S.H. Payne, and L. Paša-Tolić, H aloferax volcanii archaeosortase is required for motility, mating, and C-terminal processing of the S-layer glycoprotein. Molecular microbiology 88 (2013) 1164-1175.
[32] M.F. Abdul Halim, S. Schulze, A. DiLucido, F. Pfeiffer, A.W. Bisson Filho, and M. Pohlschroder, Lipid Anchoring of Archaeosortase Substrates and Midcell Growth in Haloarchaea. mBio 11 (2020) e00349-20.

[33] R.N. Esquivel, and M. Pohlschroder, A conserved type IV pilin signal peptide H-domain is critical for the post-translational regulation of flagella-dependent motility. Molecular microbiology 93 (2014) 494-504.
[34] M. Cerletti, M.J. Martínez, M.I. Giménez, D.E. Sastre, R.A. Paggi, and R.E. De Castro, The LonB protease controls membrane lipids composition and is essential for viability in the extremophilic haloarchaeon H aloferax volcanii. Environmental microbiology 16 (2014) 1779-1792.
[35] P. Chatterjee, M. Garcia, J. Cote, K. Yun, G. Legerme, R. Habib, M. Tripepi, C. Young, D.W. Kulp, and M. Dyall-Smith, Involvement of ArlI, ArlJ, and CirA in Archaeal Type-IV Pilin-Mediated Motility Regulation. bioRxiv (2024) 2024.03. 04.583388.
[36] R.K. Hackley, S. Hwang, J.T. Herb, P. Bhanap, K. Lam, A. Vreugdenhil, C.L. Darnell, M.M. Pastor, J.H. Martin, and J.A. Maupin-Furlow, TbsP and TrmB jointly regulate gapII to influence cell development phenotypes in the archaeon Haloferax volcanii. Molecular Microbiology (2024).
[37] I.G. Duggin, C.H. Aylett, J.C. Walsh, K.A. Michie, Q. Wang, L. Turnbull, E.M. Dawson, E.J. Harry, C.B. Whitchurch, and L.A. Amos, CetZ tubulin-like proteins control archaeal cell shape. Nature 519 (2015) 362.
[38] H. Schiller, Y. Hong, J. Kouassi, T. Rados, J. Kwak, A. DiLucido, D. Safer, A. Marchfelder, F. Pfeiffer, and A. Bisson, Identification of structural and regulatory cell-shape determinants in Haloferax volcanii. Nature communications 15 (2024) 1414.
[39] C.H. Aylett, and I.G. Duggin, The tubulin superfamily in archaea, Prokaryotic Cytoskeletons, Springer, 2017, pp. 393-417.
[40] H.J. Brown, and I.G. Duggin, Diversity and Potential Multifunctionality of Archaeal CetZ Tubulin-like Cytoskeletal Proteins. Biomolecules 13 (2023) 134.
[41] R.T. de Silva, V. Shinde, H.J. Brown, Y. Liao, and I.G. Duggin, Dynamic self-association of archaeal tubulin-like protein CetZ1 drives Haloferax volcanii morphogenesis. bioRxiv (2024) 2024.04. 08.588506.
[42] H.J. Brown, M.I. Islam, J. Ruan, M.A. Baker, S. Ithurbide, and I.G. Duggin, CetZ1-dependent assembly and positioning of the motility machinery in haloarchaea. bioRxiv (2024) 2024.05. 02.592137.
[43] R.T. de Silva, M.F. Abdul-Halim, D.A. Pittrich, H.J. Brown, M. Pohlschroder, and I.G. Duggin, Improved growth and morphological plasticity of Haloferax volcanii. Microbiology (Reading) (2021).
[44] S.W. Cline, W.L. Lam, R.L. Charlebois, L.C. Schalkwyk, and W.F. Doolittle, Transformation methods for halophilic archaebacteria. Canadian Journal of Microbiology 35 (1989) 148-152.
[45] T. Allers, H.-P. Ngo, M. Mevarech, and R.G. Lloyd, Development of additional selectable markers for the halophilic archaeon Haloferax volcanii based on the leuB and trpA genes. Applied and environmental microbiology 70 (2004) 943-953.
[46] T. Allers, S. Barak, S. Liddell, K. Wardell, and M. Mevarech, Improved strains and plasmid vectors for conditional overexpression of His-tagged proteins in Haloferax volcanii. Appl Environ Microbiol 76 (2010) 1759-69.
[47] B. Schmid, P. Tripal, T. Fraaß, C. Kersten, B. Ruder, A. Grüneboom, J. Huisken, and R. Palmisano, 3Dscript: animating 3D/4D microscopy data using a natural-language-based syntax. Nature methods 16 (2019) 278-280.

[48] A. Ducret, E.M. Quardokus, and Y.V. Brun, MicrobeJ, a tool for high throughput bacterial cell detection and quantitative analysis. Nature microbiology 1 (2016) 1-7.

[49] J. Schindelin, I. Arganda-Carreras, E. Frise, V. Kaynig, M. Longair, T. Pietzsch, S. Preibisch, C. Rueden, S. Saalfeld, and B. Schmid, Fiji: an open-source platform for biological-image analysis. Nature methods 9 (2012) 676.

[50] J. Babski, K.A. Haas, D. Nather-Schindler, F. Pfeiffer, K.U. Forstner, M. Hammelmann, R. Hilker, A. Becker, C.M. Sharma, A. Marchfelder, and J. Soppa, Genome-wide identification of transcriptional start sites in the haloarchaeon Haloferax volcanii based on differential RNA-Seq (dRNA-Seq). BMC Genomics 17 (2016) 629.

[51] M. Cerletti, M.I. Gimenez, C. Troetschel, D.A. C, A. Poetsch, R.E. De Castro, and R.A. Paggi, Proteomic Study of the Exponential-Stationary Growth Phase Transition in the Haloarchaea Natrialba magadii and Haloferax volcanii. Proteomics 18 (2018) e1800116.

[52] S. Laass, V.A. Monzon, J. Kliemt, M. Hammelmann, F. Pfeiffer, K.U. Forstner, and J. Soppa, Characterization of the transcriptome of Haloferax volcanii, grown under four different conditions, with mixed RNA-Seq. PLoS One 14 (2019) e0215986.

[53] M. Patro, I.G. Duggin, S.V. Albers, and S. Ithurbide, "Influence of plasmids, selection markers and auxotrophic mutations on Haloferax volcanii cell shape plasticity". Front Microbiol 14 (2023) 1270665.

[54] Z. Li, Y. Kinosita, M. Rodriguez-Franco, P. Nußbaum, F. Braun, F. Delpech, T.E. Quax, and S.-V. Albers, Positioning of the motility machinery in halophilic archaea. MBio 10 (2019) e00377-19.

[55] S. Ithurbide, R.T. de Silva, H.J. Brown, V. Shinde, and I.G. Duggin, A vector system for single and tandem expression of cloned genes and multi-colour fluorescent tagging in Haloferax volcanii. Microbiology 170 (2024).

[56] M. Petro, S. Sivabalasarma, S. Gfrerer, M. Rodriguez-Franco, P. Nusbaum, S. Ithurbide, and S.V. Albers, MinD2 regulates cell shape and motility in the archaeon *Haloferax volcanii*. Under review (2024).